

Camera and Laser Scanner Co-detection of Pedestrians

Hao LI, Ming YANG, Huijia QIAN

ABSTRACT—Intelligent vehicle technology is a promising technology for enhancing urban traffic safety and efficiency. Pedestrian detection is an important issue for applications of intelligent vehicles in urban environments. The kind of most widely used method for pedestrian detection is vision based method. One general problem for vision based method is how to efficiently locate a proper ROI (region of interests) which contains a candidate object. Another problem is how to detect and segment features of candidate objects out of ROI. In this paper, a camera and laser scanner co-detection method is proposed. First, a method of camera and laser scanner co-calibration is presented. Second, a method of how to obtain proper ROI and the contours of candidate objects using the co-calibration results is introduced. Finally, a decision rule is induced from a set of examples of contour shapes of both pedestrians and landmarks (They are most likely to be confused with each other because of their similarity in size). Some experimental results are given for validating the camera and laser scanner co-detection method.

1 Introduction

Intelligent vehicle technology is a promising technology for enhancing urban traffic safety and efficiency. Since there are lots of pedestrians in urban environments, the problem of how to ensure the safety of pedestrians arises urgently in the application of intelligent vehicles in urban environments. To ensure the safety of pedestrians, the intelligent vehicle system should detect pedestrians nearby correctly and in time. Therefore, pedestrian detection is an important issue for applications of intelligent vehicles in urban environments.

The problem of pedestrian detection is a considerable challenge. For this problem, the kind of most widely used method is vision based method. Broggi et al [1] proposes a method mainly based on human shape features, especially the vertical edge symmetry and binary model, which are used to localize pedestrians' heads through stereo-vision's distance refinement. Gavrila [2] uses a method of hierarchical template matching (a lot of pedestrians' templates are needed)

based on contour figures and intensity features. Curio et al [3] presents a hybrid method architecture which integrates texture information, entropy, template matching results and etc. Shashua et al [4] presents a two-steps detection method in which the Adaboost training is used for the single-frame detection step and a final decision is made by integrating information of multi-frames. Besides vision based method, laser scanner based method has also been reported [5].

The process of pedestrian detection can be mainly divided into two steps: object localization and object classification. In the first step, candidate objects are localized (obtain ROI) and segmented out from sensor data space (segment contours of candidate objects out of ROI). In the second step, a decision on whether a candidate object is a pedestrian is made based on the decision rule. The general difficulties for vision based method are at the step of object localization, while the general difficulties for laser scanner based method are at the step of object classification. Therefore, a more robust method might be realized if both camera and laser scanner are used together and cooperate with each other.

In this paper, a new camera and laser scanner co-detection method is proposed. It mainly consists of three parts: 1) a method of camera and laser scanner co-calibration; 2) a method of how to obtain proper ROI and the contours of candidate objects using the co-calibration results; 3) a decision rule induced from a set of examples of contour shapes of both pedestrians and landmarks. The paper is organized as follows: a method of camera and laser scanner co-calibration is presented in section2; the co-detection method is proposed in section3; experimental results on the co-calibration method and co-detection method are given in section4, followed by a conclusion in section5.

2 Co-calibration of camera and laser radar

The co-calibration is to determine the geometric transform relationship between three coordinates, i.e. the laser scanner coordinate, the image coordinate and the vehicle coordinate.

2.1 The three coordinate systems

The image coordinate is a 2D rectangular coordinate, denoted by a pair (u, v) , where u, v mean the rows, columns of a pixel point.

The laser scanner used is a 2D laser scanner. The laser scanner coordinate mentioned here is a 3D rectangular coordinate, denoted by a triplet (x_p, y_p, z_p) , where the origin point O_p is at the emitting point of the laser scanner; the X_p -axis and the Y_p -axis are on the scanning plane of the laser

Hao LI is with Department of Automation, Shanghai Jiao Tong University, No.800 Dong Chuan Road, Shanghai, 200240, P.R. China (haoli@sjtu.edu.cn)

Ming YANG is with Department of Automation, Shanghai Jiao Tong University, No.800 Dong Chuan Road, Shanghai, 200240, P.R. China (MingYANG@sjtu.edu.cn)

Huijia QIAN is with Department of Automation, Shanghai Jiao Tong University, No.800 Dong Chuan Road, Shanghai, 200240, P.R. China (qianhuijia23@yahoo.com.cn)

scanner; the Z_p -axis satisfies right-hand rule with the X_p -axis and the Y_p -axis.

The vehicle coordinate is a 3D rectangular coordinate, denoted by a triplet (x_w, y_w, z_w) , where the X_w -axis and the Y_w -axis are on the ground surface; the origin point O_w is right under the front center of the vehicle; the X_w -axis is in the longitudinal direction of the vehicle while the Y_w -axis is in the lateral direction; the Z_w -axis satisfies right-hand rule with the X_w -axis and the Y_w -axis.

2.2 The calibration tool and the method of obtaining control points

Some control points are needed for the co-calibration. But the laser beam is invisible, so control points can not be determined directly and they can only be determined indirectly using certain calibration tool. The calibration tool designed is shown in Fig1(a). It is a rectangular frame with one diagonal connected. A bracket on the frame bottom corner is used to hold the rectangular frame perpendicular to the ground surface where it is put.

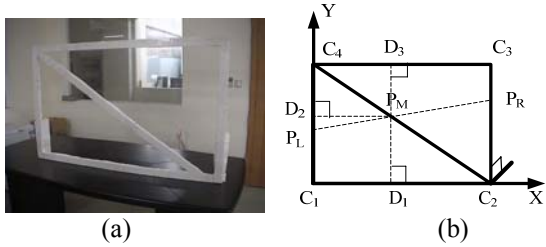


Fig 1 the calibration tool and control points

Suppose the scanning plane of the laser scanner intersects the rectangular frame at point P_L , P_M and P_R ; the line $D_3P_M D_1$ is perpendicular to C_1C_2 ; the line $P_M D_2$ is perpendicular to C_1C_4 ; as shown in Fig1(b). Although the intersected point P_M is invisible, its place can be revealed indirectly by geometric knowledge:

$$P_M D_2 = C_1 D_1 = \frac{P_L P_M}{P_L P_M + P_M P_R} C_1 C_2$$

$$P_M D_1 = C_1 D_2 = \frac{P_M P_R}{P_L P_M + P_M P_R} C_1 C_4$$

Where the lengths of C_1C_2 and C_1C_4 are measured directly and the lengths of $P_L P_M$ and $P_M P_R$ are computed from the coordinate information of P_L , P_M , P_R in the laser scanner coordinate.

If a 2D rectangular coordinate (called frame coordinate) is established on the rectangular frame of the calibration tool, as shown in Fig1(b), then the coordinates of C_1 , C_2 , C_3 , C_4 in the frame coordinate are respectively $(0,0)$, $(C_1C_2,0)$, (C_1C_2, C_1C_4) , $(0, C_1C_4)$. The image coordinates of C_1 , C_2 , C_3 , C_4 are obtained manually. The geometric transform relationship between the frame coordinate and the image coordinate can be described by a homography transform which can be computed with the coordinate information of C_1 , C_2 , C_3 , C_4 [6].

The coordinates of D_1 , P_M , D_3 in the frame coordinate are respectively $(C_1D_1,0)$, (C_1D_1, C_1D_2) , (C_1D_1, C_1C_4) . The image coordinates of D_1 , P_M , D_3 can be computed through the homography transform.

The Z_w coordinate of D_1 , P_M , D_3 in the vehicle coordinate are respectively 0, C_1D_2 , and C_1C_4 . Their X_w , Y_w coordinates in the vehicle coordinate are the same and are measured directly.

In sum, at each place where the calibration tool is put, the coordinates of P_M in the laser scanner coordinate, the image coordinate and the vehicle coordinate are all known; the coordinates of D_1 , D_3 in the image coordinate and the vehicle coordinate are known. Therefore, P_M can be used as control point for calibrating the geometric transform relationship between the laser scanner coordinate and the vehicle coordinate, while P_M , D_1 , D_3 can be used as control point for calibrating the geometric transform relationship between the vehicle coordinate and the image coordinate.

2.3 Computing the geometric transform relationship between the three coordinate systems

(a) The geometric transform relationship between the laser radar coordinate and the vehicle coordinate

Suppose there are N control points and their coordinates in the laser scanner coordinate and the vehicle coordinate are respectively (x_{pi}, y_{pi}, z_{pi}) and (x_{wi}, y_{wi}, z_{wi}) ; $i=1, 2, \dots, N$. The geometric transform between the laser scanner coordinate and the vehicle coordinate can be described by a rotation and translation transform:

$$\begin{bmatrix} \mathbf{R}_{pw} & \mathbf{T}_{pw} \\ 0 & 1 \end{bmatrix} \begin{bmatrix} x_{pi} \\ y_{pi} \\ z_{pi} \\ 1 \end{bmatrix} = \begin{bmatrix} x_{wi} \\ y_{wi} \\ z_{wi} \\ 1 \end{bmatrix} \quad (1)$$

Where \mathbf{R}_{pw} is the rotation matrix and $\mathbf{T}_{pw} = [T_x, T_y, T_z]^T$ is the translation vector. Any rotation matrix can be expressed in terms of 3 independent parameters (R_x, R_y, R_z) , i.e. $\mathbf{R}_{pw} = \exp(\mathbf{W}_R)$.

$$\mathbf{W}_R = \begin{bmatrix} 0 & -R_z & R_y \\ R_z & 0 & -R_x \\ -R_y & R_x & 0 \end{bmatrix}$$

Because of the nonlinearity of \mathbf{R}_{pw} with respect to R_x, R_y, R_z , it is not easy to compute R_x, R_y, R_z and T_x, T_y, T_z directly. An iteration method is needed to compute R_x, R_y, R_z along with T_x, T_y, T_z . Suppose the result of \mathbf{W}_R after k rounds of iteration is $\mathbf{W}_R(k)$. The initial value $\mathbf{W}_R(0)$ can be estimated quantitatively. The basic idea is: regard \mathbf{R}_{pw} as a matrix of 9 independent parameters; then a linear equation group of these 9 parameters and T_x, T_y, T_z can be derived using Eq.(1) and the coordinate information of control points; \mathbf{R}_{pw} is obtained by solving this linear equation group; then $\mathbf{W}_R(0)$ can be estimated as $(\exp^{-1}(\mathbf{R}_{pw}) - \exp^{-1}(\mathbf{R}_{pw}^T))/2$. Details are not introduced here. In fact, since the requirement of the accuracy of $\mathbf{W}_R(0)$ is not high, $\mathbf{W}_R(0)$ can be just estimated qualitatively according to the installation position of the laser scanner.

The method of refining \mathbf{W}_R with iterations is introduced as follows. Denote $R_x(k+1) = R_x(k) + \Delta R_x(k)$; $R_y(k+1) = R_y(k) + \Delta R_y(k)$; $R_z(k+1) = R_z(k) + \Delta R_z(k)$; and $\mathbf{W}_R(k+1) = \mathbf{W}_R(k) + \Delta \mathbf{W}_R(k)$. Let $\exp(\mathbf{W}_R(k) + \Delta \mathbf{W}_R(k)) \approx$

$(\mathbf{I} + \Delta\mathbf{W}_R(k))\exp(\mathbf{W}_R(k))$, and substitute it into Eq.(1)

$$\begin{bmatrix} 1 & -\Delta R_z(k) & \Delta R_y(k) \\ \Delta R_z(k) & 1 & -\Delta R_x(k) \\ -\Delta R_y(k) & \Delta R_x(k) & 1 \end{bmatrix} \begin{bmatrix} x_{pi}(k) \\ y_{pi}(k) \\ z_{pi}(k) \end{bmatrix} + \begin{bmatrix} T_x \\ T_y \\ T_z \end{bmatrix} = \begin{bmatrix} x_{wi} \\ y_{wi} \\ z_{wi} \end{bmatrix} \quad (2)$$

Where $[x_{pi}(k), y_{pi}(k), z_{pi}(k)]^T = \exp(\mathbf{W}_R(k)) [x_{pi}, y_{pi}, z_{pi}]^T$. Then from Eq.(2) it can be derived:

$$\begin{bmatrix} 0 & z_{pi}(k) & -y_{pi}(k) & 1 & 0 & 0 \\ -z_{pi}(k) & 0 & x_{pi}(k) & 0 & 1 & 0 \\ y_{pi}(k) & -x_{pi}(k) & 0 & 0 & 0 & 1 \end{bmatrix} \mathbf{U} = \begin{bmatrix} x_{wi} - x_{pi}(k) \\ y_{wi} - y_{pi}(k) \\ z_{wi} - z_{pi}(k) \end{bmatrix} \quad (3)$$

$$\mathbf{U} = [\Delta R_x(k) \quad \Delta R_y(k) \quad \Delta R_z(k) \quad T_x \quad T_y \quad T_z]^T$$

In Eq.(3), $i=1, 2, \dots, N$, so there are a total number of $3N$ equations which form a linear equation group with respect to the vector $[\Delta R_x(k), \Delta R_y(k), \Delta R_z(k), T_x, T_y, T_z]^T$ that can be obtained by solving the linear equation with least-square rule. Then $R_x(k+1), R_y(k+1), R_z(k+1)$ can be computed. After several rounds of iteration, R_x, R_y, R_z and T_x, T_y, T_z will converge; then the rotation matrix \mathbf{R}_{pw} and the translation vector \mathbf{T}_{pw} are obtained.

(b) The geometric transform relationship between the vehicle coordinate and the image coordinate

Suppose there are N control points and their coordinates in the vehicle coordinate and the image coordinate are respectively (x_{wi}, y_{wi}, z_{wi}) and (u_i, v_i) ; $i=1, 2, \dots, N$. The geometric transform between the vehicle coordinate and the image coordinate can be described by a perspective transform [6]:

$$\mathbf{M}_{wf} [x_{wi} \quad y_{wi} \quad z_{wi} \quad 1]^T = \beta [u_i \quad v_i \quad 1]^T \quad (4)$$

Where \mathbf{M}_{wf} is the perspective matrix which can be computed by solving a linear equation group using the coordinate information of the control points [6]. It is worth noting that all the image coordinates mentioned in the paper are distortion removed. So the perspective transform shown in Eq.(4) works well.

3 Co-detection of pedestrians

The architecture of the co-detection method consists of four parts: 1) cluster and sift; 2) obtaining ROI; 3) obtaining contour edges; 4) decision. First, the range data are clustered and those clusters which might represent pedestrians (the object that such cluster represents is called candidate object) are sifted out; then proper ROI is obtained using the range data of candidate objects and the co-calibration results; after that edge-extraction is carried out in ROI and contour edges of candidate objects are obtained with the help of the range data of candidate objects and the co-calibration results; finally, decision on whether a candidate object is a pedestrian is made according to the feature of its contour edges.

3.1 Cluster and sift

The cluster rule is generally described as [7]: if $\|(x_{p,i}, y_{p,i}) - (x_{p,i+1}, y_{p,i+1})\| < D_{thd}$, then the i -th and $(i+1)$ -th scanning point of laser scanner are in the same cluster; otherwise they are in different clusters. Here, $D_{thd} = K_1 \min\{\|(x_{p,i}, y_{p,i})\|, \|(x_{p,i+1}, y_{p,i+1})\|\}$, $K_1 = k \sin(\Delta\alpha/2)$; $\Delta\alpha$ is the angle resolution of

laser scanner, k is a constant chosen according to experience.

Suppose there are totally N clusters C_1, C_2, \dots, C_N ; for any cluster C_i : $\{(x_{p,n(i-1)}, y_{p,n(i-1)}), (x_{p,n(i-1)+1}, y_{p,n(i-1)+1}), \dots, (x_{p,n(i)-1}, y_{p,n(i)-1})\}$, its diameter $d(C_i)$ is defined as: $d(C_i) = \max\{\|(x_{p,j}, y_{p,j}) - (x_{p,l}, y_{p,l})\|; j, l \in [n(i-1), \dots, n(i)-1]\}$; $i=1, 2, \dots, N$. Since the size of a pedestrian's body is limited, a range $[D_{min}, D_{max}]$ is set to sift the clusters according to their diameter. If and only if the diameter of a cluster is in this range, then this cluster is reserved, and the object that such cluster represents is called candidate object; otherwise this cluster is discarded. Above, set $D_{min}=0.15\text{m}$, $D_{max}=1.2\text{m}$.

3.2 Obtaining ROI

Given a candidate cluster C_i : $\{(x_{p,n(i-1)}, y_{p,n(i-1)}), (x_{p,n(i-1)+1}, y_{p,n(i-1)+1}), \dots, (x_{p,n(i)-1}, y_{p,n(i)-1})\}$ ($z_i=0$), its two end-points are $C_L(x_{p,n(i-1)}, y_{p,n(i-1)}, z_{p,n(i-1)})$ and $C_R(x_{p,n(i)-1}, y_{p,n(i)-1}, z_{p,n(i)-1})$. The coordinates of C_L and C_R can be computed using Eq.(1), denote them as $C_L^w(x_{w,n(i-1)}, y_{w,n(i-1)}, z_{w,n(i-1)})$ and $C_R^w(x_{w,n(i)-1}, y_{w,n(i)-1}, z_{w,n(i)-1})$. A pedestrian's body could be roughly represented by a vertical rectangular envelop, as shown in Fig2(a); the four corners are denoted as BC_1, BC_2, TC_1 and TC_2 . Suppose C_L^w and C_R^w are respectively on the left and right side of the rectangular envelop; then the coordinates of these four corners in the vehicle coordinate are $BC_1(x_{w,n(i-1)}, y_{w,n(i-1)}, 0)$, $BC_2(x_{w,n(i)-1}, y_{w,n(i)-1}, 0)$, $TC_1(x_{w,n(i-1)}, y_{w,n(i-1)}, H_{max})$ and $TC_2(x_{w,n(i)-1}, y_{w,n(i)-1}, H_{max})$, where H_{max} denotes the height limit of human beings (set $H_{max} = 2.5\text{m}$). The rectangular envelop is expanded a bit (for example 30 cm) on both left side and right side.

The coordinates of the corresponding points of $C_L^w, C_R^w, BC_1, BC_2, TC_1, TC_2$ in the image coordinate can be computed using Eq.(4); their image coordinates are denoted respectively as $C_L^I(u_{CL}, v_{CL}), C_R^I(u_{CR}, v_{CR}), BC_1^I(u_{BC1}, v_{BC1}), BC_2^I(u_{BC2}, v_{BC2}), TC_1^I(u_{TC1}, v_{TC1}), TC_2^I(u_{TC2}, v_{TC2})$. The ROI should at least contain $BC_1^I, BC_2^I, TC_1^I, TC_2^I$; if a smallest vertical rectangle is chosen as the ROI, then its four corners are $(u_{min}, v_{min}), (u_{min}, v_{max}), (u_{max}, v_{min}), (u_{max}, v_{max})$; where $u_{min} = \min\{u_{BC1}, u_{BC2}, u_{TC1}, u_{TC2}\}$, $u_{max} = \max\{u_{BC1}, u_{BC2}, u_{TC1}, u_{TC2}\}$, $v_{min} = \min\{v_{BC1}, v_{BC2}, v_{TC1}, v_{TC2}\}$, $v_{max} = \max\{v_{BC1}, v_{BC2}, v_{TC1}, v_{TC2}\}$. As shown in Fig2, (b) shows the original image while (c) shows the extracted ROI of several candidate objects using above method.



Fig 2 the rectangular envelope and the region of interest (ROI)

3.3 Obtaining contour edges

Edge-extraction is carried out in ROI using Canny method [8]. In ideal condition, $C_L^I(u_{CL}, v_{CL})$ and $C_R^I(u_{CR}, v_{CR})$ should be exactly on the left and right contour edge of candidate object. Actually, there will always be a slight deviation because of all kinds of errors. $\{(u_{CL}, v_{CL}), (u_{CR}, v_{CR})\}$

are matched with edge points in ROI using closest point or iterative closest point method, and two edge points on the left and right contour edges of candidate object are obtained. Then carry out edge point connection from these two edge points until discontinuity appears or the edge direction begins to deviate largely from vertical direction (on the consideration that the contour edges of a pedestrian are generally vertical). The extracted contour edges of several candidate objects are shown in Fig3.

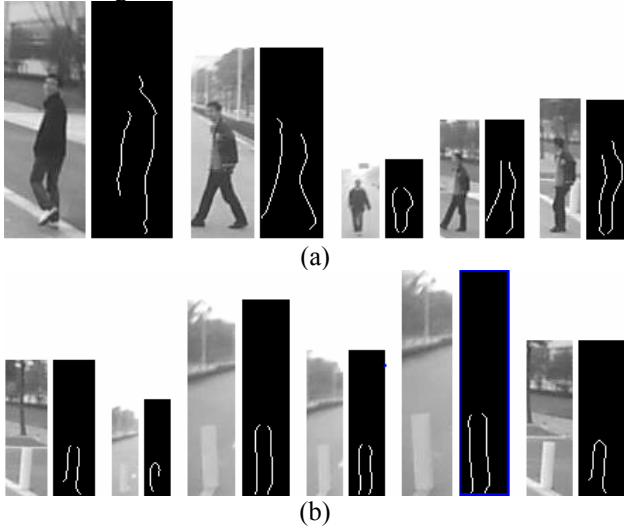


Fig 3 the contour edges of candidate objects

3.4 Decision

In this section, a decision rule is induced from a set of examples of contour shapes of candidate objects. Besides pedestrians themselves, the most likely candidate objects sifted from range data are landmarks, because of their similarity in size to pedestrians; as shown in Fig3. Therefore, the decision rule in some sense is a rule of how to distinguish pedestrians from landmarks.

A noticeable feature of landmarks is that their contour edges are almost straight on image, while the contour edges of pedestrians are irregular curved lines. A contour curve measure F_{curve} is defined as follows to describe the curved extent of contour edges of a candidate object.

Suppose the set of edge points on the left and on the right contour edge of the candidate object are respectively the set CL: $\{(u_{1,L}, v_{1,L}), (u_{2,L}, v_{2,L}), \dots, (u_{m,L}, v_{m,L})\}$ and the set CR: $\{(u_{1,R}, v_{1,R}), (u_{2,R}, v_{2,R}), \dots, (u_{n,R}, v_{n,R})\}$. Line $l_{CL}: a_{CL}u + b_{CL}v + c_{CL} = 0$ and line $l_{CR}: a_{CR}u + b_{CR}v + c_{CR} = 0$ are the straight lines fitted respectively to the edge points in set CL and in set CR with least square rule. The contour curve measure F_{curve} is defined as:

$$F_{curve} = \sqrt{\frac{\sum_{i=1}^m d((u_{i,L}, v_{i,L}), l_{CL})^2 + \sum_{j=1}^n d((u_{j,R}, v_{j,R}), l_{CR})^2}{m+n}} \quad (5)$$

Where $d((u_{i,L}, v_{i,L}), l_{CL})$ denotes the distance between point $(u_{i,L}, v_{i,L})$ and line l_{CL} ; $d((u_{j,R}, v_{j,R}), l_{CR})$ denotes the distance between point $(u_{j,R}, v_{j,R})$ and line l_{CR} .

A number of 500 samples of pedestrians and landmarks

are chosen; the contour edges of each object are extracted and the contour curve measure is computed using Eq.(5). The statistic result of F_{curve} is shown in Fig4. It shows the probability distribution of the contour curve measure of sample pedestrians and landmarks. As it can be seen from Fig4 that there is an apparent dividing line ($F_{curve}=1$) between the distribution of pedestrians and landmarks. So the decision is induced as: if $F_{curve} > 1$, then the candidate object is regarded as a pedestrian; otherwise, it is regarded as a landmark.

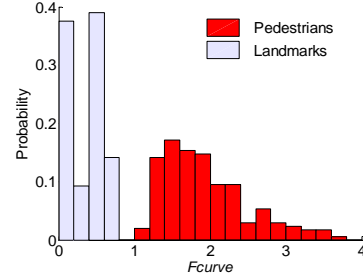


Fig 4 the probability distribution of the contour curve measure

4 Experiment

4.1 Experiment on the co-calibration method

Choose an arbitrary flat ground as the calibration field, as Fig5; put the calibration tool at several places in the calibration field and obtain the coordinate information of control points using the method introduced in section 2.2; compute the rotation matrix R_{pw} and the translation vector T_{pw} in Eq.(1) and the perspective matrix M_{wf} in Eq.(4) using the method introduced in section 2.3. Although the frame showed here happens to be roughly perpendicular to vehicle axis, it is not necessary to put the frame this way.



Fig 5 the calibration field

In order to examine the effect of the co-calibration method, each scanning point and part of laser beams are projected onto the image using the range data and the co-calibration results, thus forming a kind of augmented reality effect, as shown in Fig6. As it can be seen from Fig6, the projection matches well with the scenario, especially note that at each boundary of two neighboring objects, there is a

corresponding discontinuity in the projection of laser beam. Fig6 displays a kind of lifelikeness as if one can really see the laser beams and how they scan the scenario. Such lifelikeness indirectly testifies the effectiveness and accuracy of the proposed co-calibration method.

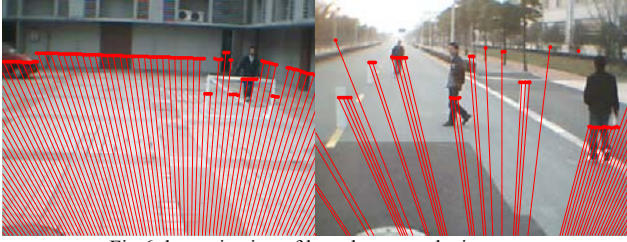


Fig 6 the projection of laser beam on the images

4.2 Experiment on the co-detection method

The intelligent vehicle used is the CyberC3 vehicle developed by the IV Lab of SJTU, with a 2D laser scanner SICK installed on the front of the vehicle and an off-the-shelf Logitech camera installed on the top of the vehicle. The camera and laser scanner are co-calibrated with the proposed method introduced in section2. The experiment scenario for pedestrian detection is shown in Fig7; the intelligent vehicle is moving on a road and its detection area is within 20m ahead and within 4m on two sides. Several pedestrians and landmarks appear in the detection area early or late during the experiment process. Every time the vision data and range data are recorded at the same time and the sample interval is about 0.1 second; every frame of recorded data is processed using the proposed co-detection method. Several images are displayed as example, shown in Fig7. A detected pedestrian is marked by bold yellow box while a detected landmark is marked by thin blue box, as shown in Fig7; it can be seen that the proposed method works well; the pedestrians as well as landmarks are correctly detected. During the whole experiment process, the omission detection ratio (omission detection means all the cases when the pedestrian is not detected or is detected as other object) and the false detection ratio (false detection means all the cases when a non-pedestrian is detected as a pedestrian) for pedestrians are respectively 1% and 3%.

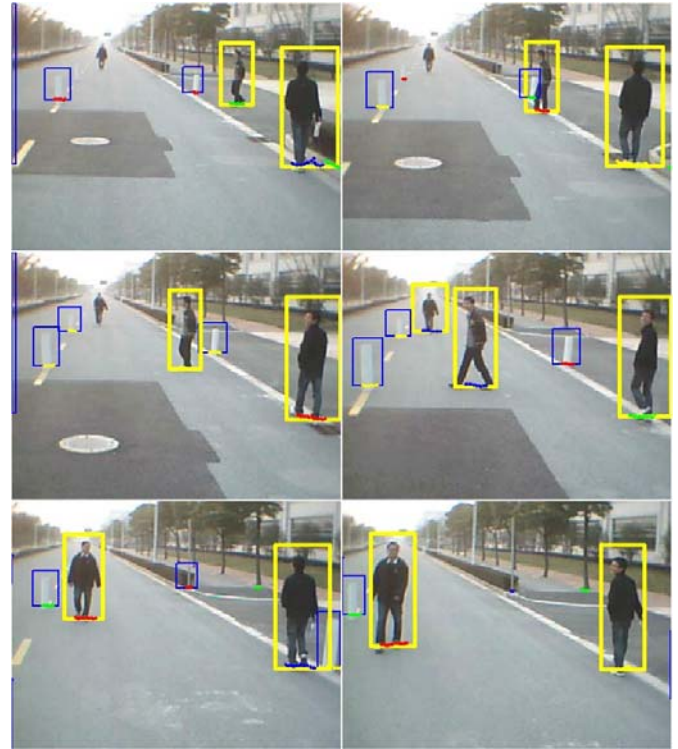


Fig 7 the result of co-detection of pedestrians

5 Conclusion

In this paper, a new co-detection method using camera and laser scanner is proposed for pedestrian detection. First, a method of camera and laser scanner co-calibration is proposed, including how to obtain coordinate information of control points and how to compute the geometric transform relationship between the laser scanner coordinate, the vehicle coordinate and the image coordinate. Then a laser scanner and camera based pedestrian detection method using the co-calibration result is proposed, including how to sift candidate objects through range data, how to obtain proper ROI and contour edges of candidate objects using range data and co-calibration result, and how to make a decision on candidate object according to its contour feature. Experiments validate the efficiency of the proposed co-calibration method and co-detection method. In future work, more sophisticated image processing method such as SVM, NN, SIFT will be integrated into the architecture of the proposed co-detection method.

Acknowledgement

This research is supported by the European CyberCars-2 project (FP6-028062) and the Shanghai Science Committee Foundation for the Mountaineering Action Plan (062107035).

Reference

- [1] Broggi A, Bertozzi M, Fascioli A, Sechi M. Shape-based pedestrian detection. In: Proceeding of IEEE Intelligent Vehicles Symposium, Dearborn, USA. IEEE, 2000, pp.215~220

- [2] Gavrila. D M, Pedestrian detection from a moving vehicle. In: Proceedings of the 6th European Conference on Computer Vision-Part II. London, UK: Springer-Verlag, 2000, pp.37~49
- [3] Curio C, Edelbrunner J, Kalinker T, Tzomakas C, Wernervon Seelen, Walking pedestrian recognition, IEEE Transactions on Intelligent Transportation Systems, 2000,1(3): 155~163
- [4] Shashua A, Gdalyahu Y, Hayun G, Pedestrian detection for driving assistance systems: single-frame classification and system level performance. In: Proceedings of IEEE Intelligent Vehicles Symposium, Parma, Italy, IEEE, 2004, pp.1~6
- [5] Tons M, Doerfler R, Meinecke M M, Obojski M A, Radar sensors and sensors platform used for pedestrian protection in the EC-funded project SAVE-U. In: Proceedings of IEEE Intelligent Vehicles Symposium. Parma, Italy. IEEE, 2004, pp.813~818
- [6] Zhang Z., Flexible camera calibration by viewing a plane from unknown orientations, in: Proceedings of 7th IEEE International Conference on Computer Vision, Corfu Greece, 1999, pp.666-673
- [7] Cristiano Premebida, Urbano Nunes. Segmentation and geometric primitives extraction from 2D laser range data for mobile robot applications. Robotica 2005 – Actas do Encontro Científico, pp.17-25
- [8] Canny J., A computational approach to edge detection, IEEE Transactions on Pattern Analysis and Machine Intelligence, 1986, 8(6): 679-698